Chemical Engineering & Processing: Process Intensification 159 (2021) 108242

Contents lists available at ScienceDirect

Chemical Engineering and Processing - Process Intensification

journal homepage: www.elsevier.com/locate/cep

Effect of isopropanol co-product on the long-term stability of TiO_2 nanoparticle suspensions produced by microwave-assisted synthesis

Enrico Paradisi [a], Roberto Rosa [b], Giovanni Baldi [c], Valentina Dami [c], Andrea Cioni [c], Giada Lorenzi [c], Cristina Leonelli [a,*]

[a] Department of Engineering "Enzo Ferrari" (DIEF), University of Modena and Reggio Emilia, Via Pietro Vivarelli, 10, 41125, Modena, IT, Italy
[b] Department of Sciences and Method for Engineering, University of Modena and Reggio Emilia, via Giovanni Amendola, 2, 42122, Reggio Emilia, IT, Italy
[c] Ce.Ri.Col. Colorobbia Research Centre, Colorobbia Consulting S.R.L., Via Pietramarina, 123, 50053, Sovigliana-Vinci (Fi), IT, Italy

ARTICLE INFO

Keywords:
TiO_2 suspension
Long-term stability
Microwave irradiation
Sol-gel synthesis
Suspension stability
Nanocrystals

ABSTRACT

In this paper we evaluate the effect of isopropanol arising from the reagent $Ti(O\text{-}iPr)_4$ on the long-term stability of nanoparticle size of TiO_2 produced during a microwave assisted sol-gel synthesis. Different configurations of microwave apparatus have been considered: the synthesis was carried out both in vessel or flask, and both performing or not isopropanol distillation through a modified microwave apparatus. Results revealed that isopropanol distillation after a short reaction time provided suspensions with slightly smaller particle size, that also show longer stability over time, especially for syntheses carried out at certain temperatures. Reactions performed distilling isopropanol from vessel and flasks showed comparable results, superior to the corresponding suspensions obtained without distilling isopropanol. This study is intended to provide a useful contribution to those applications where the need for stable TiO_2 suspensions is critical.

1. Introduction

TiO_2 is the most widely used white pigment in the world [1]. It is employed in many industrial sectors such as paint and varnishes, ceramics, plastic and paper additive, pharmaceuticals and many others [2]. The discovery of photocatalytic properties of nanosized TiO_2 [3], prompted the scientific community to further study this material for many applications, such as fuel generation [4], dye-sensitized solar cells [5], water treatment [6], sensors [7], pharmaceuticals [8] and coatings [9]. Coatings based on TiO_2 are used in many sectors, exploiting UV protection and/or photocatalytic performance of nanosized material. Having stable suspensions over time is crucial for the production of nanosized photocatalytic coatings [10]. Therefore, it's very important to study how suspension stability over time can vary due to different synthesis parameters [11]. In literature, many papers examine the stability of TiO_2 suspensions [12–18], and several are concerned with long-term stability [19–32]. Results show that the latter is influenced by many factors like nanoparticle concentration [12,15,17–20,23,29,26–30], pH of solution [13–15,17–22,24,25,29,26–30], presence of surfactants [14,25,28,32], the kind of solvent [15,16,19,18–20] and others [33]. Many of these studies involve suspensions created *ex-post*, having a commercially available TiO_2 powder which is later suspended in a liquid medium, to carry on studies [25,26–30]. For industrial applications, it would yet be much more favorable having a stable TiO_2 suspension directly produced as a result of the nanoparticle synthesis. The idea is to protect workers from direct contact with the nanotitania powders by adopting a wet process, also reducing the process time involved.

A way to do so is represented by sol-gel synthesis. The sol-gel route to nano TiO_2 is widely studied in academic literature [34–39] due to operational simplicity and to the ability to control several nanoparticle features, such as particle [38,40] or pore size [39,41] and morphology [38,42,43]. In sol-gel synthesis usually a titanium alkoxide precursor is used as titanium source and the synthesis is carried out in water, with the addition of an acid as catalyst for peptization and a surfactant in order to control nanoparticle size [36,37]. In this method, depending on the initial concentration, a considerable amount of the corresponding alcohol is also formed as co-product, which actually becomes part of the solvent mixture, maybe having an influence on suspension stability over time. Anyway, this fact is mainly neglected in the academic literature to the best of our knowledge, despite several papers discussing the long-term stability in sol-gel TiO_2 synthesis [12–24], only one accounts

* Corresponding author.
E-mail address: cristina.leonelli@unimore.it (C. Leonelli).

https://doi.org/10.1016/j.cep.2020.108242
Received 13 August 2020; Received in revised form 20 November 2020; Accepted 25 November 2020
Available online 1 December 2020

for the effect of alcohol derived from the parent alkoxide [19].

Among the technologies employed in sol-gel synthesis, microwave heating has emerged as a powerful tool to reduce synthesis times [44] and save power [45] for greener synthesis [46]. Many synthesis procedures have appeared in literature in order to get nanoparticles with different features [47,48] but long-term stability studies on the obtained suspensions are still lacking.

Finally, some papers report the distillation of the alcoholic co-product deriving from parent titanium alkoxide in a sol-gel synthesis [19,49,50]. None of them was dealing with microwaves used as heating source during the synthesis step [51] and even in these cases long term stability was not thoroughly investigated.

In this context, pursuing our work in microwave assisted synthesis [52,53], a study on how isopropanol deriving from Ti(O-*i*Pr)$_4$ can affect TiO_2 nanoparticle suspension stability over time was also explored. To do so, we investigated the long-term stability of nanosized TiO_2 suspensions produced *via* sol-gel microwave alkoxide hydrolysis, comparing as-prepared samples with samples where isopropanol was removed by microwave distillation. Our original investigation intends to provide a useful contribution to those applications where the need for stable TiO_2 suspensions in storage and/or in use is critical.

2. Experimental section

2.1. Microwave system used and its modifications for isopropanol distillation

2.1.1. MW oven modifications to distill isopropanol

The native microwave system was a Milestone ETHOS ONE system supplied with dedicated vessels. In order to distil isopropanol, a vacuum pump with a proper condensation system was installed and connected to the microwave oven. The evaporation and condensation system was set-up as in a classic evacuation system for organic synthesis. The plastic-made joint usually attached to the pressure sensor was found to be suitable for the connection of pipes leading solvent vapours to the condenser both inside and outside the oven Fig. 1a and b (**1**)). In this way the external part of the system can be left untouched, while the internal configuration can be switched from vessel to flask when necessary. A mechanical stirrer can be installed above the instrument and the agitation rod can be inserted from the main MW hole located in the upper part of the instrument (Fig. 1a and b (**2**)). The mechanical stirrer is fixed with rubber bands, as seen in Fig. 1b.

2.1.2. Modifications to carry out reactions in flask

To carry out reactions in a three-necked flask, the original ETHOS ONE rotating plate was disassembled, and a base made of refractory materials was placed below the flask. A soft refractory material was used to avoid flask breaking under the strong mechanical agitation. The system was fixed with rubber bands to the refractories in such a way that makes movement impossible during stirring (Fig. 1c). This system combines robustness and a bit of flexibility, to avoid accidental breaking under mechanical stirring due to the agitation rod of the mechanical stirrer coming from above (Fig. 1a and c (**2**)). The probe used in this configuration was the native ETHOS ONE thermocouple, placed above the reaction mixture through a side neck, in such a way that it does not touch the liquid (Fig. 1a and c (**3**)). For this purpose, a special home-made joint was created with a Pasteur and two rubber septa: these were chosen because the system must tolerate vacuum (Fig. 1a and c (**4**)). A simple vacuum joint and pipe are then connected to the original plastic-made pressure joint through the third neck.

2.1.3. MW oven modifications to carry out reactions in vessel

For reactions carried out in the vessel we used a special vessel that can be equipped with temperature and pressure probes. In this case, the temperature probe was an optical fiber (Fig. 2a and b (**1**)), while, in place of the native connection to pressure probe, a hollow screw cap connected to larger pipes was used (Fig. 2a, and b (**2**)). Its tail was brought to the pressure joint which brings vapours to the outer part of the system, previously described in section 2.1.1 (Fig. 2a, (**3**)). This was necessary because the native connection cable to the pressure probe was too small and isopropanol distillation was found not to be effective. An O-ring was used to ensure vacuum sealing in the vessel (Fig. 2b (**4**)).

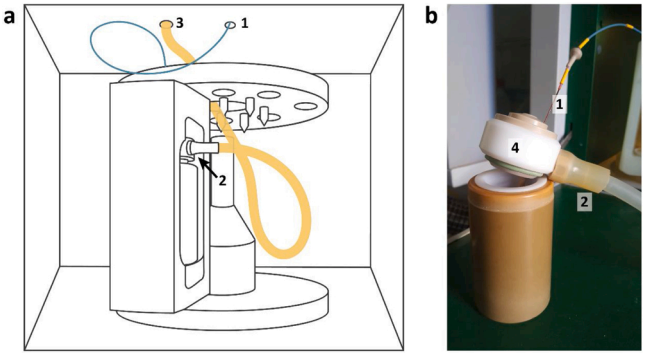

Fig. 2. a: schematic representation of the ETHOS one MW system modified to distill isopropanol from a vessel. **1**: optical fiber inlet; **2**: modified vessel connection with the outside, which made distillation possible; **3**: to vacuum. b: detail of the vessel used in experiments, with modifications. **1**: the optical fiber is placed in the hole of the special vessel; **2**: detail of the homemade connection pipes leading solvent vapors to the distillation apparatus; **4**: a rubber O-ring was added to the internal part of the vessel's lid to ensure vacuum.

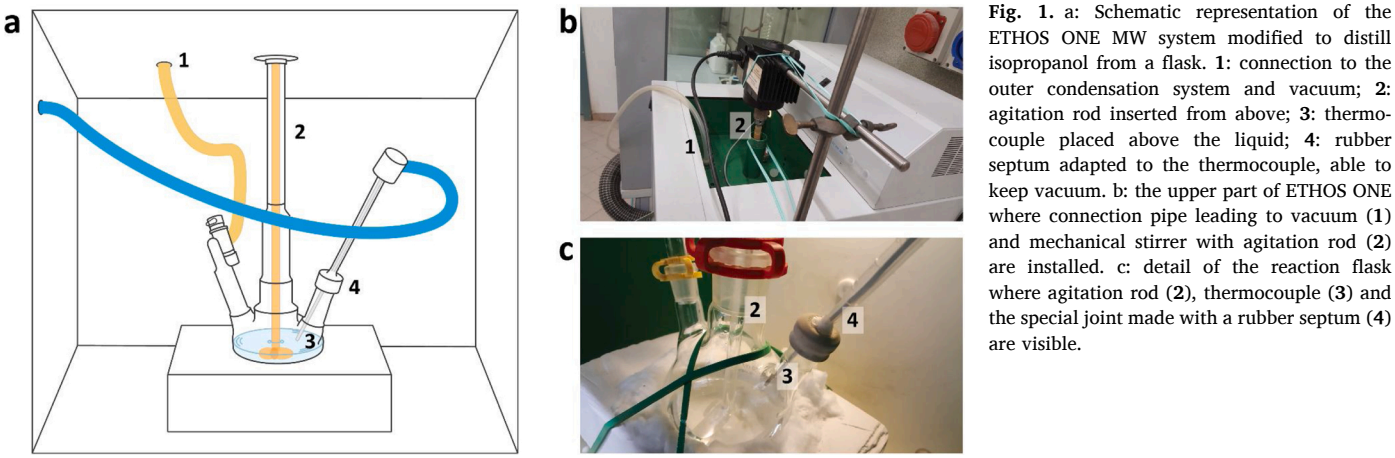

Fig. 1. a: Schematic representation of the ETHOS ONE MW system modified to distill isopropanol from a flask. **1**: connection to the outer condensation system and vacuum; **2**: agitation rod inserted from above; **3**: thermocouple placed above the liquid; **4**: rubber septum adapted to the thermocouple, able to keep vacuum. b: the upper part of ETHOS ONE where connection pipe leading to vacuum (**1**) and mechanical stirrer with agitation rod (**2**) are installed. c: detail of the reaction flask where agitation rod (**2**), thermocouple (**3**) and the special joint made with a rubber septum (**4**) are visible.

2.2. Materials

$Ti(O\text{-}iPr)_4$ (technical grade), and a premixed acidic mixture were provided by Colorobbia Consulting S.R.L. The acidic mixture was an aqueous HCl solution (technical grade) with a small amount of a surfactant named TRITON X-100 (Sigma Aldrich, laboratory grade). The amounts of the three components present in the mixture are based on a known procedure used to get a commercially available product [54], and were as following:

32 % HCl = 3.1 %

Bi-distilled water = 96.9 %

Triton X-100 = 0.013 %.

This Acidic Mixture, mentioned hereafter as AM, has been optimized in the patented procedure [54].

2.3. Procedures for TiO_2 nanoparticle synthesis

2.3.1. Procedure for TiO_2 nanoparticle synthesis in flask

A 250 mL three necked flask was filled with 77 mL of AM and fixed to its support inside the MW oven. The stirring rod was introduced into the flask and fixed to the mechanical stirrer. The temperature probe was introduced in a side neck and fixed appropriately. Mechanical stirring was then set to 400 rpm, then $Ti(Oi\text{-}Pr)_4$ (25 mL) was dropwise added with a pipette over 10 min under stirring. The connection to the outer distillation apparatus was then fixed, the oven was closed, and the following microwave treatment was operated:

- 5 min of heating to the desired temperature, max MW power: 300 W.
- 30 min of holding at the desired temperature, max MW power: 300 W.
- 5 min of cooling.

Then the oven was opened, the probe removed, and 15 mL of the crude reaction mixture were taken in a Falcon tube and stored without further modification. The samples collected in this way are named F_TiO_2_XX_ND, where XX is reaction temperature. Temperatures used were 50 °C, 60 °C, 70 °C and 80 °C. Then, the probe was attached again to the flask and the reaction mixture was warmed up at 50 °C with the aid of microwaves, the vacuum pump was switched on, and the solvent was distilled *in vacuo* (30 min, 50 °C, 300 W, 400 rpm). After solvent distillation the volume was reduced to 30−40 mL, and the mixture was transferred into a beaker. The reaction flask and rod were washed with an appropriate amount of bi-distilled water and washings were gathered with the mixture in the beaker to obtain a milky suspension at 6% TiO_2 w/w. The so-obtained mixture was magnetically stirred 0.5−1 h to improve homogeneity, and then stored with the name F_TiO_2_XX_D without further modification.

2.3.2. Procedure for TiO_2 nanoparticle synthesis in vessel

The MW vessel was filled with 38.4 mL of AM and then $Ti(Oi\text{-}Pr)_4$ (12.4 mL) was added dropwise over 5 min under vigorous magnetic stirring (approx. 800 rpm). A large amount of white precipitate was formed immediately. The vessel was transferred to the MW oven and then subjected to a cycle of MW heating with subsequent stirring, which will be mentioned hereafter as “run”. The run was as follows.

- 2 min of heating to the desired temperature, max MW power: 200 W.
- 5 min of holding at the desired temperature, max MW power: 200 W.
- 2 min of cooling.
- 5 min of magnetic stirring outside of the microwave.

This run was repeated six times for an overall holding time of 30 min at the desired temperature. Temperatures used were 50 °C, 60 °C, 70 °C and 80 °C. In most of the cases, the reaction mixture became a thick gel during the runs, but after the stirring stage it had returned to a liquid appearance and was finally obtained as a turbid suspension. The samples that did not require isopropanol distillation were simply stored in Falcon tubes and used for DLS analysis without further modifications. Such samples are named V_TiO_2_XX_ND where XX is the reaction temperature. Otherwise, the mixture was subjected to the following isopropanol distillation procedure. The solvent was distilled *in vacuum* at 50 °C using MW as the heating source. The mixture was heated to 50 °C (5 min, 300 W). Then, vacuum pump was switched on and distillation was prolonged at the same maximum power for 30 min or to complete dryness. The resulting material appeared as off-white crystals or as a white slurry, depending on the case. This material was then re-suspended in 50 mL of bi-distilled water to give a milky suspension at 6% TiO_2 w/w, stored in Falcon tubes and used for DLS analysis without further modifications. Such samples are named V_TiO_2_XX_D where XX is the reaction temperature.

2.4. Analytical techniques used

2.4.1. Size distribution

Nanoparticle size distribution was evaluated with Dynamic Light Scattering (DLS) using a Malvern Panalytical Zetasizer S nano ZS instrument. The obtained 6% w/w TiO_2 suspensions were diluted 1:100 vol/vol with bi-distilled water before analysis and quickly shaken manually in a volumetric flask. One mL of diluted sample was then transferred in a Malvern disposable polystyrene cuvette (DTS0012) which was placed into the instrument. Each measurement was performed using the following parameters:

Material: Polystyrene latex

Dispersant: Water

Temperature: 25 °C

Measurement angle: 173° backscatter

Number of measurements: 5

Number of runs per measurement: 10 runs of 10 s each.

Results are expressed in Z-Average, the % error in most cases varies between 1 and 15 %.

2.4.2. XRD

The crystalline phase composition of the TiO_2 suspensions was determined by X-ray powder diffraction (XRD) using a Philips X’PERT PRO instrument. The obtained 6% w/w TiO_2 suspensions were dried at 100 °C before analysis. Each measure was performed using the following parameters:

Angle range: 3.000–140.000 °

Step size: 0.00167113°

Time for step: 20.32 s

Scan speed: 0.104445 (°/s)

Run timer: 00:22:26

Rietveld refinement method was used to quantify the percentages of anatase, rutile and brookite and the associated crystal parameters such as crystallite size.

2.4.3. TEM

The microstructure of the TiO_2 nanoparticles was determined by TEM observations at acceleration voltage of 20 kV (Talos™ F200S G2, Thermo Fisher Scientific, Waltham, MA, USA), equipped with a patented, integrated X-ray energy dispersive spectroscopy (EDS) system with two silicon drift detectors (SDD) for superior sensitivity and elemental mapping capabilities of up to 105 spectra/sec. The samples were prepared by placing a drop of the obtained suspension on common Formvar® coated copper grids, followed by drying and carbon coating to enhance the resolution of the scanning micrograph obtained. The stability of the specimen material under the scanning electron beam was checked comparing the surface morphology before and after the focusing process. This assured that the originality of the structure, pattern, contour and texture of the nanoparticles were not affected by any physical and chemical distortion before and during the TEM analysis.

2.5. Photocatalytic tests

The photocatalytic activity of TiO_2 coatings was verified by using a device designed and developed by Ce.Ri.Col. Colorobbia Research Centre, Colorobbia Consulting S.R.L., Italy (Fig. 3a) [55]. The system consists of a glass reaction chamber equipped with a quartz window, in which the environmental conditions are simulated in terms of concentration of contaminants, temperature and relative humidity. The device works automatically. Dedicated software controls the flow of pollutant gas and the moisture. The photocatalytic efficacy was tested studying nitric oxides (nitrogen monoxide and/or nitrogen dioxide) degradation using a chemiluminescence NO-NO_2-NO_x analyzer (Model 42i, Thermo Fisher). The sample was placed inside the chamber and irradiated with light sources having different spectral properties on the base of the characteristics of the titanium dioxide nanoparticles.

The photoreactors allows performing the analysis in two different modes:

- Continuous mode;
- Discontinuous mode.

The first mode allows to perform the analysis in single passage from the reaction chamber directly to the chemiluminescence analyzer. In this case, the inlet pollutant concentration remains constant during the entire analysis. The initial value is determined before switching-on the light. After turning on the light, a decrease of pollutant concentration is measured, which is proportional to the efficiency of the photocatalyst.

In the second mode, the reaction chamber is connected to a bag and to a peristaltic pump, in order to create a closed circuit. The bag works as reservoir from which it is possible to send the pollutant atmosphere to the measuring instrument. Regulating the sampling and the recirculation times, it is possible to obtain data to determine the kinetic of the degradation reaction.

2.5.1. Sample preparation

The samples were prepared applying the suspension on a marble slab with $10 \times 10 \times 1$ cm^3 dimensions using a brush. The amount of material applied was around 1.15−1.20 g. The samples were dried in oven at 50 °C before the photocatalytic test.

2.5.2. Test execution

To perform the photocatalytic tests, discontinuous mode was used.

The specimens were introduced in the photoreactor chamber and the analysis was carried out by mixing dry air, moist air and the selected pollutant in proportions such as to obtain a fixed concentration of pollutant in an atmosphere having about 50 ± 10 % of relative humidity at a temperature of about 25 ± 5 °C. The pollutant used was NO and the initial value of NO concentration was 500 ± 50 ppbv.

Considering that all the samples contained pristine undoped titanium dioxide, it was decided to use a lamp with ultraviolet component (Ultravitalux, Osram) and the light spectrum is reported in Fig. 3b. At the distance of 12 cm between the light and the sample inside the chamber of photoreactor, the irradiance was 50 W/m^2.

Before starting the photooxidation reaction, the reactor was purged with pure air.

The results of NO depletion are expressed as percentage and not as concentration: in this way the data are independent from the initial value of NO concentration.

3. Results

3.1. Reactions without isopropanol distillation: comparison between vessel and flask

Fig. 4 reports the results for the TiO_2 mean nanoparticle size obtained through DLS over an aging time of 90 days for the four sets of samples described in the experimental section. Fig. 4a shows the results for the reactions carried out in vessels, without a subsequent isopropanol distillation. All the reactions carried out at temperatures between 50 °C and 80 °C show very large nanoparticle sizes in the first days of aging (out of scale in the plot) and 3–6 days are necessary for the samples to get to low size values. Then, two pairs of reactions with opposite behavior can be identified. Reactions at 50 °C and 60 °C quickly reach low size values (around 25 nm). Later on, a particle enlargement starts, very quickly in the case of V_TiO_2_50_ND, more slowly in the case of V_TiO_2_60_ND, sufficient to declare particles size of this material unstable over time. The two reactions performed at 70 °C and 80 °C, instead, show a slightly slower decrease rate in particles size (especially V_TiO_2_80_ND), but then we observed a stable behavior in long-term aging. These materials show sizes of 30−35 nm at the end of the considered aging time. The best of these reactions can be considered V_TiO_2_70_ND, due to its relatively fast decreasing sizes to around 30 nm and further stability at this value over time.

Fig. 4b shows results for the same reactions, carried out in flask. Even in this case all the reactions produced particles having high size values in the first days of aging (out of scale in the plot), and required 3–5 days to reach values below 80 nm size. The fastest decrease, anyway, is again shown by the reactions carried out at 50 °C and 60 °C (F_TiO_2_50_ND, F_TiO_2_60_ND). Between day 10 and 40, all reactions show oscillations in size values, but at day 40 they all have size values around 25 nm, except F_TiO_2_80_ND, that shows a roughly double size. From that moment on, anyway, the two reactions carried out at 50 °C and 60 °C show a particles size enlargement, as it happened in reactions carried out in vessel, and even the particles enlargement rate have the same

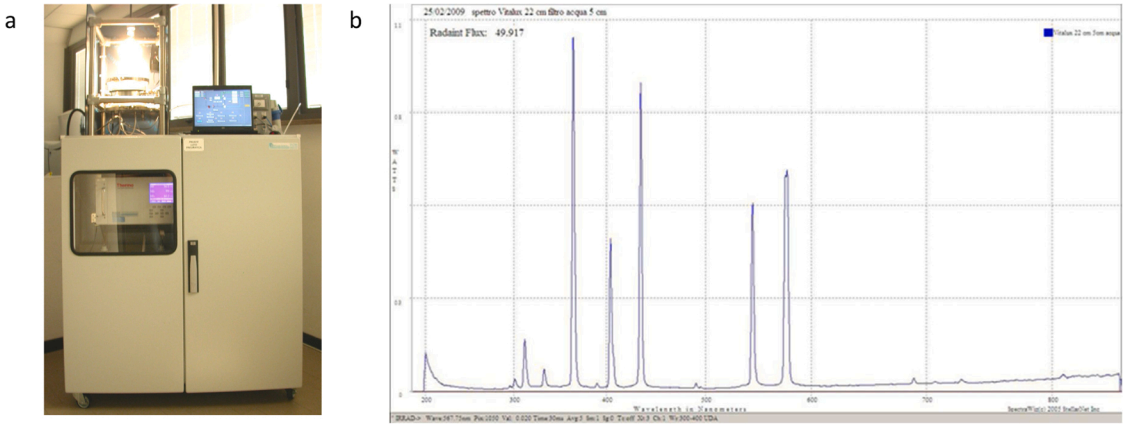

Fig. 3. landscape picture of the photoreactor (a, left) and Ultravitalux lamp light spectrum (b, right).

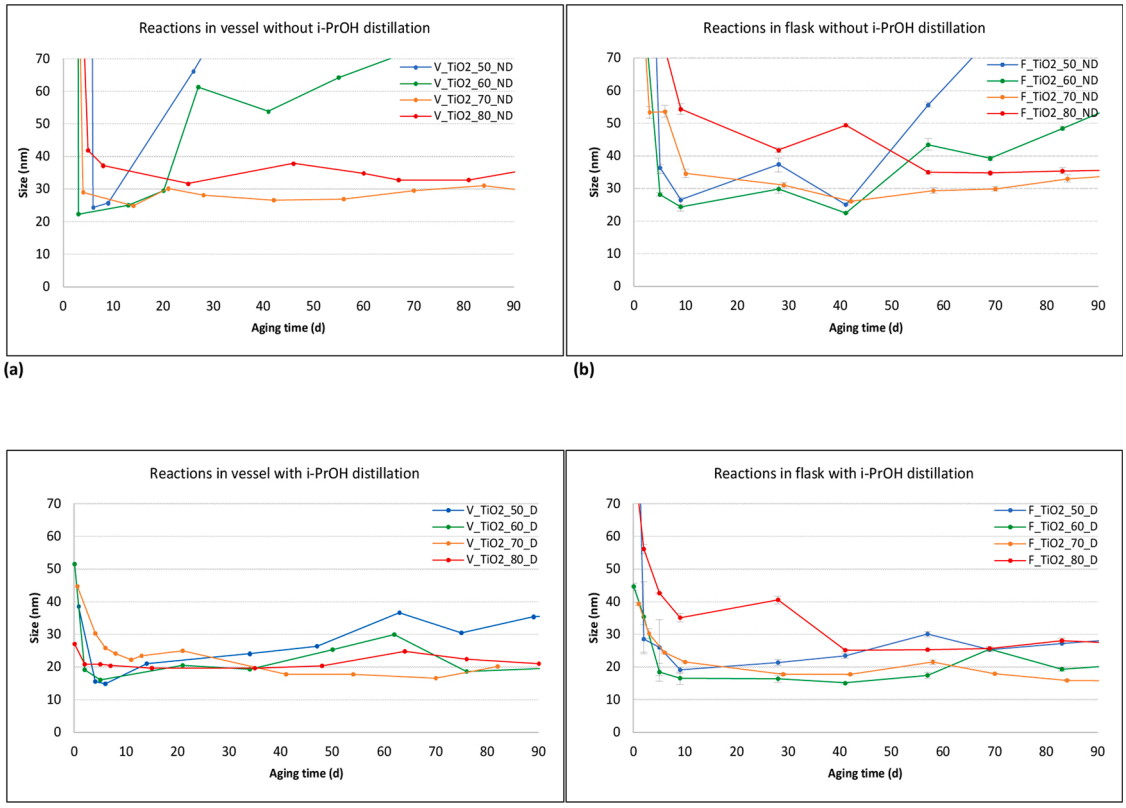

Fig. 4. Mean particle size diameter over aging time of TiO_2 nanoparticles obtained performing MW-assisted reactions in: (a) vessel without any further treatment; (b) flask without any further treatment; (c) vessel with subsequent isopropanol distillation; (d) flask with subsequent isopropanol distillation.

trend, with the reaction carried out at 50 °C enlarging faster respect to the one carried out at 60°. Conversely, F_TiO_2_80_ND starts decreasing in size, reaching 35 nm of mean particle size at the end of the considered aging time, a value similar to F_TiO_2_70_ND, that gave the most stable suspension and can be considered the best reaction even in this case. Therefore, despite times are longer, the case of reactions performed in flask without a subsequent isopropanol distillation shows the same trend of the vessel case, with all the reactions showing high values of particles size in the beginning followed by a relatively fast decrease, but with the products of reactions carried out at 50 °C and 60 °C that at a later time start enlarging, while products of reactions carried out at 70 °C and 80 °C are stable or decrease in size.

3.2. *Reactions with isopropanol distillation: comparison between vessel and flask*

Fig. 4c and d show the results of reactions carried out at the same four temperatures and in the same conditions respect to Fig. 4a and b, but with subsequent isopropanol distillation after 30 min of reaction time. Comparing the plots reported in Fig. 4a and c, the difference in the results of reactions carried out in vessels, with and without isopropanol distillation stands out. Respect to the previous case, data in Fig. 4c show a smaller nanoparticle size since the beginning of aging time. Even here shrinking is observed in the first aging days, and in this case sizes are lower (15−25 nm) if compared to the previous one (22−37 nm). Moreover, all the reactions show particles size stability over all the considered aging time, and at the end of aging all show size values around 20 nm, with the only exception of sample V_TiO_2_50_D that enlarges, but reaches only 35 nm. Therefore, these data clearly show that distillation of isopropanol arising from the parent Ti(O-*i*Pr)$_4$ has been beneficial for the reaction outcome, both considering absolute particle size, nanoparticle stability and the size shown right after the end of the synthesis (first points of traces in Fig. 4c). This means that this procedure could be useful both for those researchers or manufacturers who need a small TiO_2 particle size and for those that need a suspension stable over a long time. Results are even more valuable if considering that particle size is very small (in most of the cases below 30 nm) somewhat irrespectively of reaction temperature.

Fig. 4d shows the results of aging over time for reactions carried out in flask with subsequent isopropanol distillations: procedures are comparable with those used for vessel synthesis regarding reaction times, and the same as seen in Fig. 4b concerning the first part of the reaction. If we compare results in Fig. 4d and b, we observe that, even in this case, as happened with vessels, particles size is generally lower performing isopropanol distillation, respect to the sizes shown by unmodified reactions. Times needed to reach the smallest size are similar, as many reactions need 10 days to reach a low value, even if a couple of them (F_TiO_2_60_ND and F_TiO_2_70_D) show quite small sizes since the beginning of the aging, being also the most stable ones concerning particles size. Reaction performed at 80 °C has a surprisingly similar trend when compared to the one where isopropanol distillation was not carried out, while reaction carried out at 50 °C is much more stable over time, even if its trend is increasing at the end of aging. Samples F_TiO_2_60_D and F_TiO_2_70_D can be considered the reactions with the best results in this group, having a stable particles size over all aging time and still being below 20 nm of mean particle size at the end of aging. At this time, even the remaining two reactions show sizes lower than 30 nm. Also in the case of flask, it can be concluded that isopropanol distillation is beneficial for the long-term stability of particle sizes in TiO_2 suspensions. Moreover, as recorded for vessels, even for the reactions carried out in flask the absolute values of size are lower in case of isopropanol distillation. At the end of aging, all reactions in Fig. 4d show values below 30 nm, while without isopropanol distillation all reactions show values above 30 nm.

Comparing reactions where isopropanol distillation was performed (Fig. 4c and d), the large difference is represented by sample

F_TiO_2_80_D, which shows much higher values respect to the corresponding reaction carried out in vessel, especially at the beginning. Another slight difference is the time needed for products to reach the lowest size, which is slightly longer in the case of flask. Product sizes are comparable, except for the reaction carried out at 80 °C, but probably the most convenient procedure for operational simplicity is performing the reaction in flasks.

3.3. Results of X-ray powder diffraction

Fig. 5a and b exhibit the XRD patterns of the TiO_2 powders collected from the suspensions named V_TiO_2_70_D and F_TiO_2_70_D after the drying process. The observed diffraction peaks match with those of the three mineralogical phases of titania, in a good agreement with the JCPDS cards of anatase (ICDD PDF No:21-1272), brookite (ICDD PDF No:29-1360) and rutile (ICDD PDF No:21-1276).

Both samples are characterized by the presence of the three phases and by the low crystallinity grade. To better understand the differences in the mineralogical composition, the amounts of the individual phases and the value of the crystal sizes were calculated using the Rietveld refinement technique, which fits a calculated profile (including all structural and instrumental parameters) to experimental data.

The values of the percentages of anatase, brookite and rutile and the associated crystal size are reported in Table 1. As can be seen from the table, the two samples do not show relevant differences in term of percentage of crystalline phases, being for both samples anatase and brookite the major components with traces of rutile. The crystal size clearly indicates the nanometric nature of the products, with particularly large crystals for brookite in V_TiO_2_70_D sample. Given the complexity of Rietveld refinement, the data in Table 1 could be affected by error of about 20–30 %.

3.4. TiO_2 nanoparticles morphology at TEM

Crystallite dimensions obtained by diffraction analysis were compared with the data collected with particle size distributions calculated using TEM images (Fig. 6). There is a good agreement between the values obtained by means of the two experimental techniques: being the primary particle grain size in the range 5–10 nm, average value of 4.57 ± 1.068 nm (std dev), in the TEM images (Fig. 6). HR-TEM images show the high crystallinity of all TiO_2 nanopowders as from the high occurrence of fringe patterns and rings in the electron diffraction patterns.

3.5. Results of photocatalytic tests

The photocatalytic activity of the samples has been evaluated in the NO oxidation reaction using an experimental apparatus previously reported [55]. The results of NO depletion are expressed as percentage over time. Fig. 7 shows the trend of two different marble surfaces prepared respectively with sample V_TiO_2_70_D (red line in Fig. 7) e F_TiO_2_70_D (blue line in Fig. 7), compared with Colorobbia commercial titanium dioxide suspension named PH000025, applied according the method indicated in paragraph 2.5.1. The sample F_TiO_2_70_D achieved more than 60 % NO removal in 100−105 min, very similar to the activity of PH000025. Therefore, we have been able to produce, using a fast microwave synthesis, a material having the same photocatalytic activity of the commercially available product PH000025, remarkably reducing its synthesis times. Similar results were found in literature [56] adopting a fixed-bed reactor at atmospheric pressure and room temperature by feeding 2800 mL/min of the reaction mixture (NO/air, 100 ppb of NO, 315-400 nm spectral range, of 7.5 W/m^2, sample weight of 50 mg). The catalytic efficiency is expressed in terms of conversion % of NO, calculated with the following equation:

$$\text{Conversion } \% = (C_{in} - C_{min}/\ C_{in}) * 100 \quad (1)$$

where C_{in} is the initial concentration of NO and C_{min} is the minimal concentration of NO.

The results of the application of the Eq. (1) to sample PH000025, V_TiO_2_70_D and F_TiO_2_70_D are reported in Table 2.

Table 1
Crystal size and mineralogical composition of the investigated TiO_2 samples.

Sample	Anatase wt%	Crystal size (nm)	Brookite wt%	Crystal size (nm)	Rutile wt%	Crystal size (nm)
V_TiO_2_70_D	63	6	28	55	9	5
F_TiO_2_70_D	70	5	27	4	3	8

4. Discussion

Results are here discussed to extract some general trends on the influence of the distillation step on the particle size of the nanotitania suspensions during an observation time of 3 months.

Reactions without isopropanol distillation need 3–6 days to reach low particle size values. This timing is in accordance with results previously published for conventional heating reactions [19–21]. Vorkapic and Matsoukas reported similar shrinking times to get the smallest particle size for TiO_2 suspensions prepared *via* acid hydrolysis of titanium alkoxides [20,20,21]. The mechanism reported in that paper involves a fast (seconds) agglomeration process to very large aggregates, followed by a relatively slow peptization (days) and very slow (weeks) particle growth. Our microwave reactions without isopropanol distillation generally follow this trend, with the exception that reactions

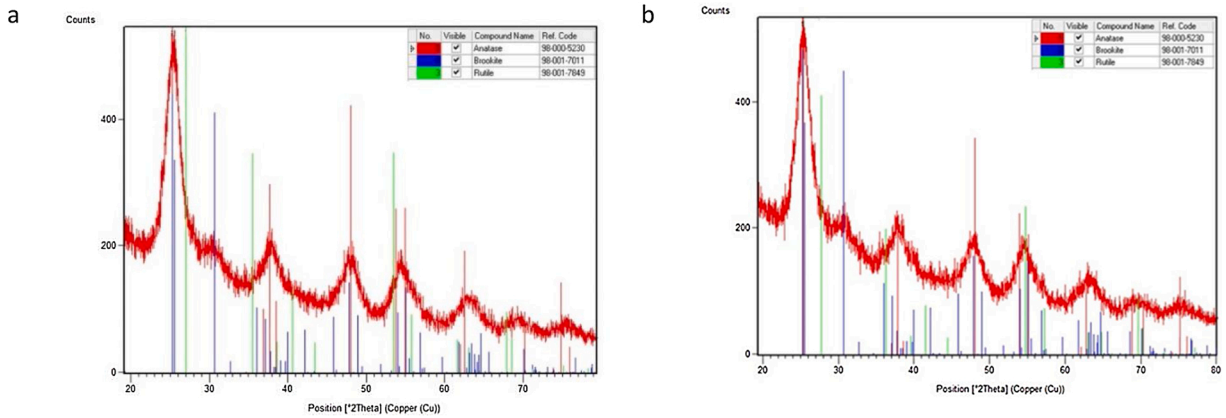

Fig. 5. XRD spectra of powder of: (a, left) sample V_TiO_2_70_D; (b, right) sample F_TiO_2_70_D.

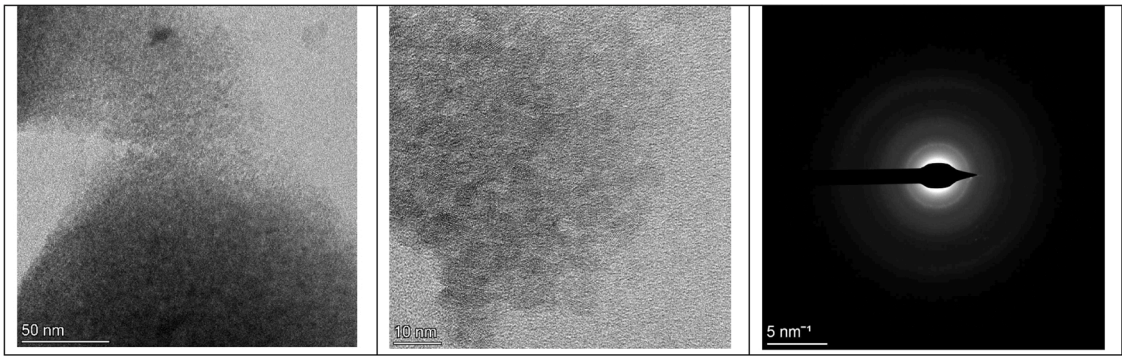

Fig. 6. TEM bright field image of powder of sample F_TiO$_2$_70_D at low enlargements (left), high magnification (centre) and electron diffraction (right).

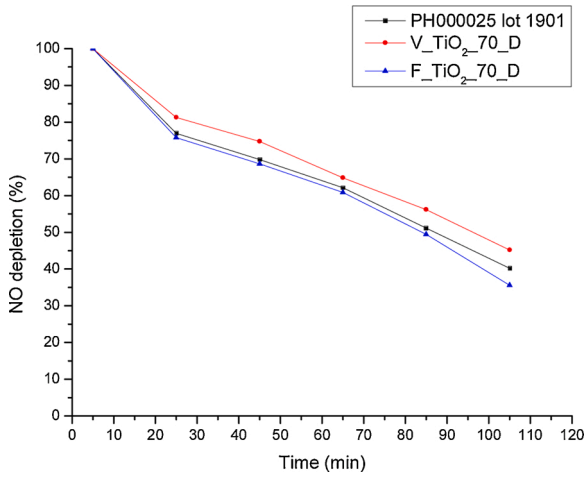

Fig. 7. NO depletion for the samples V_TiO$_2$_70_D e F_TiO$_2$_70_D, compared with Colorobbia commercial product PH000025.

Table 2
Photocatalytic efficiency of the investigated TiO_2 samples presented as conversion % of NO.

Sample	Conversion (%)
PH000025	59.8
V_TiO$_2$_70_D	54.8
F_TiO$_2$_70_D	64.4

performed at 50−60 °C initiate a fast agglomeration at some point. This effect is not very clear at the moment, unless a deep influence of the solvent is involved. Vorkapic and Matsoukas reported also a detrimental alcoholic solvent effect on TiO_2 suspensions during peptization, which lowers dielectric constant and ionic strength. This effect seems to influence more the final nanoparticle size rather than the actual stability of suspension [20]. The same and other papers [17–19,24] report the stability of TiO_2 suspensions to be mainly influenced by the amount of acid used during peptization, in our case this parameter was never varied. Therefore, what we observe must be due to the influence of reaction temperature. It must be noted that our procedure for stirring requires the opening of MW vessels repeatedly, and that, for safety reasons, reactions carried out in flasks were not completely sealed. Isopropanol, therefore, might have been evaporated from reaction environment. Of course, at the highest the reaction temperature, the highest amount of isopropanol might have been removed. Another factor that should be considered is that, giving our short reaction times, actual hydrolysis might be incomplete [24]: as a result, the process slowly goes on during peptization. In this case, additional isopropanol would be released over time, and this would destabilize the suspension at some point. This event would of course be more marked at low synthesis temperatures. These two combined effects could ascribe for the better stability of suspensions synthesized at higher temperatures without isopropanol distillation (Fig. 4).

Since alcohol influence on stabilization and final nanoparticle size is reported, it is not surprising that our reactions with isopropanol distillation show a slightly smaller size respect to the others. In all our reactions, particle size reduction occurs in the first 3–6 days of aging, so a slow peptization mechanism is also active in our case. Anyway, isopropanol removal seems to speed up this mechanism, producing particles having relatively small in size, which then further decrease to the minimum dimensions in an easier way. It is also highly likely that isopropanol distillation increases reaction rate, simply according to Le Chatelier's principle. Isopropanol removal seems to favor suspension stability over time producing suspensions which are stable at low size values for several months (Fig. 4). The obtained primary particles are an efficient mixture of titania crystalline phases that shows similar results as those recorded in literature by Degussa P25 product with a value of 66 for the conversion % of NO under UV irradiation [56].

In any case, results obtained from our study follow some general trends already shown for reactions carried out in conventional syntheses as reported by literature, so a specific non-thermal microwave effect can reasonably be excluded.

5. Conclusions

The influence of isopropanol, as a by-product from the parent Ti(O*i*-Pr)$_4$ hydrolysis, on the long-term stability of TiO_2 suspensions obtained through microwave assisted sol-gel synthesis was studied by DLS over an aging time of 90 days. Syntheses were performed both in vessel and in flask for 30 min at temperatures between 50 °C and 80 °C for unmodified samples. Applying subsequent *in situ* isopropanol distillation for samples was made possible by attaching an adequate vacuum and condensation apparatus to the MW oven.

Results highlight the influence of isopropanol on the long-term stability of the obtained suspensions. Both in vessel and flask some suspensions containing isopropanol (reactions carried out at 50° and 60 °C) were found to become unstable after 10–20 days in the case of vessel, and after 40 days in the case of flask.

Isopropanol distillation proved to be beneficial both for reactions carried out in vessel and flask. Suspensions show a lower mean particle size, in many cases very low since the beginning of the aging, and stable all over the considered aging time. Results obtained in vessel seem more uniform, but results of reactions carried out in flask are also remarkable. Perhaps this approach should be preferred due to its operational simplicity.

Remarkably, the most stable and smaller in size of these materials, F_TiO$_2$_70_D, showed comparable results with a commercially available product in photocatalytic tests, meaning that this catalyst could be

effectively synthesized in a fast, simple, cost-effective and operator-friendly manner. One of the most interesting aspects of the approach followed in this work is the idea of producing the ready to use suspension in a one pot synthesis and alcohol distillation procedure. Such an approach can be eventually adopted in a continuous flow microwave reaction and can be valuable for industrial implementation [57].

In this way we offer to the scientific community and industrial manufacturers a simple way to obtain stable crystalline nanotitania suspensions in a wide range of temperatures and with two different modes, providing a versatile tool to synthesize TiO_2 suspensions which might be useful for coating applications.

CRediT authorship contribution statement

Enrico Paradisi: Conceptualization, Methodology, Investigation, Validation, Resources, Data curation, Writing - original draft. **Roberto Rosa:** Formal analysis, Visualization, Writing - review & editing, Supervision. **Giovanni Baldi:** Supervision, Project administration, Funding acquisition. **Valentina Dami:** Methodology, Investigation, Validation, Resources, Data curation. **Andrea Cioni:** Validation, Resources, Data curation. **Giada Lorenzi:** Methodology, Investigation. **Cristina Leonelli:** Conceptualization, Writing - review & editing, Visualization, Supervision, Project administration, Funding acquisition.

Declaration of Competing Interest

The authors report no declarations of interest.

Acknowledgments

The project leading to this publication has received funding from the European Union's Horizon 2020 research and innovation programme under grant agreement No 820716.

EP and LC are grateful to Dr. Miriam Hanuskova and Prof. Tiziano Manfredini for their kind permission of the use of DLS instrument as well as to Eng. Joseph Cross for English language editing and to Gregorio Vaccari for the graphic design of schemes.

Authors acknowledge CIGS "Centro Interdipartimentale Grandi Strumenti" staff, specifically Dr. Mauro Zapparoli and Dr. Massimo Tonelli, for offering access to their instruments and helpful expertise.

References

[1] M.C.F. Karlsson, R. Álvarez-Asencio, R. Bordes, et al., Characterization of paint formulated using secondary TiO2 pigments recovered from waste paint, J. Coat. Technol. Res. 16 (2019) 607–614.
[2] M.J. Gázquez, J.P. Bolívar, R. Garcia-Tenorio, F. Vaca, A review of the production cycle of titanium dioxide pigment, Mater. Sci. Appl. 5 (2014) 441–458.
[3] A. Fujishima, K. Honda, Electrochemical photolysis of water at a semiconductor electrode, Nature 238 (1972) 37–38.
[4] Y. Ma, X. Wang, Y.Jia X. Chen, H. Han, C. Li, Titanium dioxide-based nanomaterials for photocatalytic fuel generations, Chem. Rev. 114 (2014) 9987–10043.
[5] Y. Bai, I. Mora-Seró, F. De Angelis, J. Bisquert, P. Wang, Titanium dioxide nanomaterials for photovoltaic applications, Chem. Rev. 114 (2014) 10095–10130.
[6] G. Iervolino, I. Zammit, V. Vaiano, L. Rizzo, Limitations and prospects for wastewater treatment by UV and visible-light-Active heterogeneous photocatalysis: a critical review, Top. Curr. Chem. 378 (2020) 7.
[7] J. Bai, B. Zhou, Titanium dioxide nanomaterials for sensor applications, Chem. Rev. 114 (2014) 10131–10176.
[8] T. Rajh, N.M. Dimitrijevic, M. Bissonnette, T. Koritarov, V. Konda, Titanium Dioxide in the service of the biomedical revolution, Chem. Rev. 114 (2014) 10177–10216.
[9] K. Liu, Moyuan Cao, A. Fujishima, L. Jiang, Bio-inspired titanium dioxide materials with special wettability and their applications, Chem. Rev. 114 (2014) 10044–10094.
[10] K.E. Varner, K. Rindfusz, A. Gaglione, E. Viveiros, Nano Titanium Dioxide Environmental Matters: State of the Science Literature Review, U.S. Environmental Protection Agency, Washington, DC, 2010. EPA/600/R-10/089.
[11] Z.R. Ismagilov, L.T. Tsykoza, N.V. Shikina, V.F. Zarytova, V.V. Zinoviev, S. N. Zagrebelnyi, Russ. Chem. Rev. 78 (2009) 873–885.
[12] Eric A. Barringer, H. Kent Bowen, High-purity, monodisperse TiO_2 powders by hydrolysis of titanium tetraethoxide. 1. Synthesis and physical properties, Langmuir 1 (1985) 414–420.
[13] Eric A. Barringer, H. Kent Bowen, High-purity, monodisperse TiO_2 powders by hydrolysis of titanium tetraethoxide. 2. Aqueous interfacial electrochemistry and dispersion stability, Langmuir 1 (1985) 420–428.
[14] A. Hernández-Gordillo, A. Hernández-Arana, A. Campero, L.I. Vera-Robles, Biomimetic sol−Gel synthesis of TiO_2 and SiO_2 nanostructures, Langmuir 30 (2014) 4084–4093.
[15] G. Oskam, A. Nellore, R.L. Penn, P.C. Searson, The growth kinetics of TiO2 nanoparticles from titanium(IV) alkoxide at high Water/Titanium ratio, J. Phys. Chem. B 107 (2003) 1734–1738.
[16] K.M.S. Khalil, T. Baird, M.I. Zaki, A.A. El-Samahy, A.M. Awad, Synthesis and characterization of catalytic titanias via hydrolysis of titanium(IV) isopropoxide, Colloids Surf. A Physicochem. Eng. Asp. 132 (1998) 31–44.
[17] J.L. Look, C.F. Zukoski, Alkoxide-derived titania particles: use of electrolytes to control size and agglomeration levels, J. Am. Ceram. Soc. 75 (1992) 1587–1595.
[18] J.L. Look, C.F. Zukoski, Colloidal stability and titania precipitate morphology influence of short-range repulsions, J. Am. Ceram. Soc. 78 (1995) 21–32.
[19] P. Alphonse, A. Varghese, C. Tendero, Stable hydrosols for TiO_2 coatings, J. Sol-Gel Sci. Techn. 56 (2010) 250–263.
[20] D. Vorkapic, T. Matsoukas, Effect of temperature and alcohols in the preparation of titania nanoparticles from Alkoxides, J. Am. Ceram. Soc. 81 (1998) 2815–2820.
[21] D. Vorkapic, T. Matsoukas, Reversible agglomeration: a kinetic model for the peptization of titania nanocolloids, J. Coll. Interface Sci. 214 (1999) 283–291.
[22] S.L. Isley, R.L. Penn, Titanium dioxide nanoparticles: effect of sol-gel pH on phase composition, particle size, and particle growth mechanism, J. Phys. Chem. C 112 (2008) 4469–4474.
[23] O. Pavlova-Verevkinaa, N. Golubkob, A. Sumbatovc, L. Ozerinad, Comparison of the long-term stability of TiO_2 hydrosols with different concentration of nanoparticles, Adv. Sci. Technol. 77 (2013) 53–58.
[24] B. Yoldas, Hydrolysis of titanium alkoxide and effects of hydrolytic polycondensation parameters, J. Mater. Sci. 21 (1986) 1087–1092.
[25] S. Chakraborty, An investigation on the long-term stability of TiO_2 nanofluid, Mater. Today: Proc. 11 (2019) 714–718.
[26] Z. Liua, T. Yina, Y. Chena, Z. Chenga, S. Moa, L. Jiaa, Improving the stability of TiO_2 aqueous suspensions by coupling TiO_2 nanoparticles on ZrP nanoplatelets, Energy Procedia 75 (2015) 2199–2204.
[27] N. Mandzy, E. Grulke, T. Druffel, Breakage of TiO_2 agglomerates in electrostatically stabilized aqueous dispersions, Powder Technol. 160 (2005) 121–126.
[28] S.H. Othman, S.A. Rashid, T.I.M. Ghazi, N. Abdullah, Dispersion and stabilization of photocatalytic TiO_2 nanoparticles in aqueous suspension for coatings applications, J. Nanomater. (2012). Article ID 718214 | 10 pages.
[29] Y. Safaei-Naeini, M. Aminzare, F. Golestani-Fard, F. Khorasanizadeh, E. Salahi, Suspension stability of titania nanoparticles studied by Uv-Vis spectroscopy method, Iran, J. Mater. Sci. Eng. 9 (2012) 62–68.
[30] N.-Y. Joo, J. Lee, S.J. Kim, S.H. Hong, H.M. Park, W.S. Yun, M. Yoon, Nam W. Song, Preparation of an aqueous suspension of stabilized TiO_2 nanoparticles in primary particle form, J. Nanosci. Nanotechnol. 13 (2013) 6153–6159.
[31] N.E. Jasbi, D. Dorranian, Effect of aging on the properties of TiO_2 nanoparticle, J. Theor. Appl. Phys. 10 (2016) 157–161.
[32] J. Veliscek-Carolan, R. Knott, T. Hanley, Effects of precursor solution aging and other parameters on synthesis of ordered mesoporous titania powders, J. Phys. Chem. C 119 (2015) 7172–7183.
[33] Effect of stirring is cited in ref. 17, effect of temperature is cited in refs 19-20.
[34] X. Chen, S.S. Mao, Titanium dioxide nanomaterials: synthesis, properties, modifications, and applications, Chem. Rev. 107 (2007) 2891–2959.
[35] Y. Wang, Y. He, Q. Lai, M. Fan, Review of the progress in preparing nano TiO_2: an important environmental engineering material, J. Environ. Sci. China (China) 26 (2014) 2139–2177.
[36] P. Nyamukamba, O. Okoh, H. Mungondori, R. Taziwa, S. Zinya, Synthetic methods for titanium dioxide nanoparticles: a review, in: Dongfang Yang (Ed.), Titanium Dioxide: Material for a Sustainable Environment, IntechOpen, 2018. ISBN: 978-1-78923-327-328.
[37] Low-temperature sol–gel synthesis of crystalline materials A. V. Vinogradov, V. V. Vinogradov, RSC Adv. 4 (2014) 45903–45919.
[38] M. Cargnello, T.R. Gordon, C.B. Murray, Solution-phase synthesis of titanium dioxide nanoparticles and nanocrystals, Chem. Rev. 114 (2014) 9319–9345.
[39] F. Petronella, A. Truppi, M. Dell'Edera, A. Agostiano, M.L. Curri, R. Comparelli, Scalable synthesis of mesoporous TiO_2 for environmental photocatalytic applications, Materials 12 (2019) 1853–1874.
[40] L. Sang, Y. Zhao, C. Burda, TiO_2 nanoparticles as functional building blocks, Chem. Rev. 114 (2014) 9283–9318.
[41] S. Bagheri a, Z.A.M. Hir, A.T. Yousefi, S.B.A. Hamid, Progress on mesoporous titanium dioxide: synthesis, modification and applications, Microporous Mesoporous Mater. 218 (2015) 206–222.
[42] M. Ge, J. Cai, J. Iocozzi, C. Cao, J. Huang, X. Zhang, J. Shen, S. Wang, S. Zhang, K.-Q. Zhang, Y. Lai, Z. Lin, A review of TiO_2 nanostructured catalysts for sustainable H_2 generation, Int. J. Hydrogen Energy 42 (2017) 8418–8449.
[43] X. Wang, Z. Li, J. Shi, Y. Yu, One-dimensional titanium dioxide nanomaterials: nanowires, Nanorods Nanobelts Chem. Rev. 114 (2014) 9346–9384.
[44] Y.-J. Zhu, Feng Chen, Microwave-assisted preparation of inorganic nanostructures in liquid phase, Chem. Rev. 114 (2014) 6462–6555.
[45] F.K. Butt, A.S. Bandarenka, Microwave-assisted synthesis of functional electrode materials for energy applications, J. Solid State Electrochem. 20 (2016) 2915–2928.

[46] V. Palma, D. Barba, M. Cortese, M. Martino, S. Renda, Eugenio Meloni, Microwaves and heterogeneous catalysis: a review on selected catalytic processes, Catalysts 10 (2020) 246–304.
[47] M. Baghbanzadeh, L. Carbone, P.D. Cozzoli, C.O. Kappe, Microwave-assisted synthesis of colloidal inorganic nanocrystals, Angew. Chem. Int. Ed. 50 (2011) 11312–11359.
[48] M.B. Schütz, L. Xiao, T. Lehnen, T. Fischer, S. Mathur, Microwave-assisted synthesis of nanocrystalline binary and ternary metal oxides, Int. Mater. Rev. 64 (2018) 341–374.
[49] A. Hosseinnia, M. Keyanpour-Rad, M. Kazemzad, M. Pazouki, A novel approach for preparation of highly crystalline anatase TiO_2 nanopowder from the agglomerates, Powder Technol. 190 (2009) 390–392.
[50] À. Ribes, S. Sánchez-Cabezas, A. Hernández-Montoto, L.A. Villaescusa, E. Aznar, R. Martínez-Máñez, M.D. Marcos, M.J. López-Tendero, S. Pradas, A. Cuenca-Bustos, Lab and pilot-scale synthesis of M_xO_m@SiC core–Shell nanoparticles, Materials 13 (2020) 649–663.
[51] A patent cites the use of microwave in a sol-gel synthesis where isopropanol was removed by distillation, but, in this case, microwaves were used in the drying step, and not during synthesis. See: S.-E. Park, J.-S. Hwang, J.-S. Chang, J.-M. Kim, D.-S. Kim, H.-S. Chai, US 6.566.300 B2, 2003, Korea Research Institute of Chemical Technology.
[52] C. Leonelli, T.J. Mason, Microwave and ultrasonic processing: now a realistic option for industry, Chem. Eng. Process. 49 (2010) 885–900.
[53] W. Lojkowski, C. Leonelli, T. Chudoba, J. Wojnarowicz, A. Majcher, A. Mazurkiewicz, High-energy-Low-Temperature technologies for the synthesis of nanoparticles: microwaves and high pressure, Inorganics 2 (2014) 606–619.
[54] G. Baldi, M. Bitossi, A. Barzanti, WO2006/061367 “Process for preparing dispersions of TiO2 in the form of nanoparticles, and dispersions obtainable with this process and functionalization of surfaces by application of TiO2 dispersions” [Colorobbia Italia S.p.A.].
[55] G. Baldi, A. Cioni, V. Dami, WO2011/016061 “Apparatus for determining the residual quantity of polluting agents in a gas mixture and process for determining such quantity” [M. Bitossi].
[56] V. Trevisan, M. Signoretto, F. Pinna, G. Cruciani, G. Cerrato, Investigation on titania synthesis for photocatalytic NOx abatement, Chimica Oggi/Chem. Today 30 (2012) 25–28.
[57] A.B. Corradi, F. Bondioli, A.M. Ferrari, B. Focher, C. Leonelli, Synthesis of silica nanoparticles in a continuous-flow microwave reactor, Powd. Technol. 167 (2006) 45–48.